

Wall slip in the molecular dynamics simulation of thin films of hexadecane

A. Jabbarzadeh,^{a)} J. D. Atkinson, and R. I. Tanner

*Department of Mechanical & Mechatronic Engineering, The University of Sydney,
New South Wales 2006, Australia*

(Received 24 February 1998; accepted 28 October 1998)

A molecular dynamics simulation of a thin liquid film as it is sheared between two planar walls is reported. The model liquid is composed of linear chain molecules of hexadecane ($C_{16}H_{34}$) with intramolecular architecture such as bond stretching, angle bending and dihedral potentials included in the model. Designing a model that can mimic the planar shear flow enables us to study important questions on the effects of the wall properties on the slip between the liquid film and the wall. Different properties of the wall such as wall density, wall stiffness and wall–fluid interaction strength have been studied to determine the slip between the wall and fluid. The slip has been investigated for strong and weak adsorbing surfaces at various shear rates. The results emphasize the importance of adsorption on the degree of slip. The dependence of slip on the film thickness is also demonstrated. © 1999 American Institute of Physics. [S0021-9606(99)51105-7]

I. INTRODUCTION

In fluid mechanics the idea of nonslip boundaries for small molecule fluids is generally accepted and is supported by experimental observations; the velocity of the fluid approaches the wall velocity close to the wall. However for polymers or short chain molecules this may not always be true especially at high shear stress.

The idea of a nonslip condition, at least for gases, lacks backing from kinetic theory.¹ Three models of the walls used by Maxwell that employ either random or elastic interaction between fluid and the wall, or a combination of both, all predict wall slip¹. There are also experimental measurements by optical techniques that predict slip for polymers which intensifies with increased shear rate.² Theoretical work by de Gennes³ suggests that polymer melts should slip on a nonadsorbing solid surface. Pearson and Petrie⁴ suggested that the boundary condition of flow near a solid surface depends on the relative size of the fluid particles, surface asperities and characteristic dimension of flow such as tube diameter or the film thickness. In other words the size of the fluid particles compared to the roughness of the wall plays a crucial role in determining the appropriate boundary condition.

In modern tribology it is believed that the thickness of lubrication film can be as thin as 10^{-9} m.⁵ So for high speed engine parts or micromachinery devices shear rates as high as 10^{10} s⁻¹ or higher can be expected. At these high shear rates molecular dynamics (MD) simulation can be used as a powerful tool to explore the properties of the fluid. Some researchers have tried to understand the crucial issue of slip by conducting MD simulations. Some of these simulations conducted for compressible fluids and gases with low density predict a slip velocity at the wall.^{6,7} However these simulations employ the “random thermal wall” because of its simplicity. There are other simulations that use structured atomic walls^{8,9} that also predict slip on the wall. A two-dimensional

MD simulation by Sun and Ebner¹ has shown that by using a structured atomic wall with long range interaction parameters combined with an inert wall one can avoid velocity slip. Their work also shows that a repulsive wall with frozen particles would give slip. Structured atomic walls are also used for the shear flow simulation of model Lennard-Jones (LJ) liquids.¹⁰ This simulation has also demonstrated the presence of slip that increases with shear rate. For more complex fluids such as polymers or shorter alkane molecules the slip would be larger and to induce high shear rates a more intricate wall may be used. Shear simulations of short chain alkane molecules such as hexadecane¹¹ confined between rigid atomic walls have shown that there is a substantial amount of slip between the wall and fluid. The slip is greatly dependant on the wall–fluid interaction and with low energetic walls a “plug flow” characterized by almost complete slip can be observed. In simulations of linear molecules of tetracosane and branched molecules of squalane by hydrocarbon walls¹² where butane chains are tethered to structureless walls the slip is also observed. In the case of tetracosane at low shear rates and temperatures plug flow was observed. This very high degree of slip is attributed to the fully extended and layered structure of the fluid molecules. In experiments with thin film liquids the shear viscosity is usually calculated from the measured shear stress and apparent shear rate which is calculated from the plate separation and velocity. This representation of the data apparently assumes a nonslip boundary condition that makes the average shear rate inside the fluid the same as the apparent shear rate. This assumption may be correct at the low shear rates (up to 10^4 s⁻¹) used in the experiments. In the simulation of chain molecules such as hexadecane we will observe that the amount of slip could be very significant. To present the results in a way comparable to the experiments one has the option to show them with respect to the actual^{11,12} shear rate which is obtained from the calculated streaming velocity profile. In this method, especially at lower shear rates, the calculated velocity profiles are prone to statistical errors and the calculated

^{a)}Electronic mail: ahmadj@mech.eng.usyd.edu.au

shear rate will not be reliable. So the calculated properties such as viscosity tend to have larger statistical uncertainties. Although it might be true that the slip is large at higher shear rates for smooth surfaces, with surfaces that more efficiently transfer the momentum from the walls to the confined fluid the slip can be smaller and even a completely nonslip boundary condition may hold. So developing a model that can economically produce results with nonslip boundary conditions is beneficial if one intends to apply a required high shear rate to the fluid by a boundary-driven method. This can be used for a comparison between the homogenous nonequilibrium molecular dynamics (NEMD) results and boundary-driven methods or for other purposes. It is also beneficial in a sense if one assumes that the results for thin film experiments are conducted under nonslip conditions. The degree of slip for short chain molecules will depend on the wall properties. So in order to design a model that gives less slip we investigate here the effect of wall properties on the wall slip. Note that we are not attempting here to accurately model the individual atoms of any particular real wall material. Rather, we seek a simple model for the wall which, upon varying the wall parameters, will provide a range of slip or nonslip conditions so as to economically investigate the effect of degree of slip on the flow.

We have already reported rheological and structural properties of thin hexadecane films obtained from these series of simulations.¹³ The current paper intends to establish the reasons in more details for choosing the wall model used here and also to analyze the slip phenomenon in particular and in more detail.

II. SIMULATION DETAILS

In this simulation the fluid is confined between two solid walls. These walls are parallel to the XY plane and Couette flow is generated by moving the walls in opposite directions along the X axis with the same speed so that shear is applied in the XZ plane. The fluid is a model polymer consisting of chain molecules. Each molecule has several interaction sites. These interaction sites, which we will refer to as ‘‘atoms,’’ are actually CH_3 or CH_2 groups connected together thus making a chain. This kind of polymer model, known as united atoms (UAs), is widely used by researchers for simulation of alkanes,¹⁴ hexadecane,^{15,16} octane,^{17,18} and polyethylene.¹⁹ The model used for the polymer chain is an extension of the Ryckart and Bellemans²⁰ model. The model includes angle bending, bond stretching and dihedral angle potentials. We have used chain molecules with 16 interaction sites as a model of hexadecane in our simulation. Hexadecane with a reduced density of $2.288 \sigma^{-3}$ is sheared

under an isothermal condition at a reduced temperature of $T=9.46 \epsilon/k_B$, where σ and ϵ are the usual Lennard-Jones length and energy parameters. Simulations are conducted at very high pressures so that the density of sheared hexadecane is slightly higher than what was used in some other simulations.¹¹ In the initial set of simulations each wall comprises three layers of atoms of a body centred cubic (bcc) lattice. Each atom on the wall is attached by a stiff spring to its lattice position. The wall springs have a potential in the form

$$\phi_s = \frac{1}{2} k_w R^2, \quad (1)$$

where k_w is the stiffness of the spring and R is the distance of the wall atoms from their lattice sites. The density of the wall atoms can be adjusted by packing them at different distances from each other. All the interactions between the atoms of different molecules and also the interactions between the atoms which belong to the same molecule and are separated with more than three atoms are governed by a 6–12 Lennard-Jones potential described by:

$$\phi_{\text{LJ}}(r) = 4\epsilon \left[\left(\frac{\sigma}{r} \right)^{12} - \left(\frac{\sigma}{r} \right)^6 \right] - \phi_{\text{shift}}, \quad (2)$$

$$\phi_{\text{shift}} = 4\epsilon \left[\left(\frac{\sigma}{r_c} \right)^{12} - \left(\frac{\sigma}{r_c} \right)^6 \right],$$

where r is the distance between two particles. For hexadecane the values of $\epsilon/k_B = 50.5$ K and $\sigma = 0.4045$ nm as recommended by Chynoweth and Michopoulos¹⁵ are used. The interaction between the wall particles and fluid particles is also governed by these equations with the wall length parameter $\sigma_w = \sigma$ but with ϵ replaced by ϵ_w which depends on the strength of interaction between the walls and fluid.

The flexibility of the chains is restricted by a bond stretching potential $\phi(r)$, a bond angle potential $\phi(\theta)$ and a torsional potential $\phi(\alpha)$.²² The parameters for these potentials are given in Table I. The mass of the interaction sites on fluid molecules and the wall atoms is equal to the mass of CH_2 which is 14.125 amu. The equations of motion for the fluid and wall particles are:

$$\begin{aligned} \dot{\mathbf{r}}_i &= \frac{\mathbf{p}_i}{m}, \\ \dot{\mathbf{p}}_i &= \mathbf{F}_i. \end{aligned} \quad (3)$$

The isothermal condition is achieved by rescaling the thermal component of the atomic velocities in all three directions according to the following equation:

TABLE I. Parameters of intramolecular potentials.

Stretching potential $\phi(r)^a$	$k = 51600 \epsilon \sigma^{-2}$	$r_0 = 0.153$ nm
Bond angle potential $\phi(\theta)^b$	$k_\theta = 868.6 \epsilon$	$\theta_0 = 109.53^\circ$
Torsional potential $\phi(\alpha)$ (kJ/mol)	$C_0 = 9.2789$ $C_1 = 12.1557$ $C_2 = -13.1201$ $C_3 = -3.0597$ $C_4 = 26.2403$ $C_5 = -31.4950$	

^aTaken from Ref. 15.

^bTaken from Ref. 21.

$$\beta^2 = (3Nk_B T_0) / \sum_{i=1}^N m_i (\mathbf{v}_i - U_i)^2, \quad (4)$$

where β is the rescaling factor by which all the thermal components of the velocities are rescaled. U_i is the flow velocity and \mathbf{v}_i is the laboratory velocity of the particle that is measured with respect to a fixed set of the coordinate system. k_B is the Boltzmann constant and T_0 is the set temperature. In our problem we have only flow or streaming velocity in the X direction. Some of the generated heat in the fluid is absorbed by the wall particles, although rescaling the thermal components of the velocities every few time steps ensures that the fluid temperature remains constant. The wall particles are also thermostatted in the same way. The streaming velocity is evaluated by a slicing technique which is described elsewhere.^{10,22} Other local quantities such as density and temperature can be calculated in a similar way. The results of the streaming velocity profile then are fitted to a fifth order polynomial given by

$$U_x(z) = \sum_{k=1}^5 C_k z^k. \quad (5)$$

The streaming velocity of particles then can be calculated from their Z coordinate.

The equations of motion are integrated by a leapfrog Verlet algorithm with a time step of 0.001 in reduced units. The simulations are performed by a parallel algorithm²² on a cluster of DEC Alpha 500/286 workstations by using the parallel virtual machine (PVM) message passing software that provided good speedup (up to 11 \times) and efficiency.

III. DEVELOPING A WALL WITH LOWER SLIP

In order to study the effect of various wall properties on slip we start with the wall that was described in Sec. II. There are several parameters that affect the slip. We have carried out several simulations with different parameters to quantify their effect on the wall slip. These parameters are mostly related to the wall properties, namely wall density (ρ_w), wall–fluid interaction strength (ϵ_w) and the wall stiffness (k_w). For all the simulations in this section the distance between two walls was 9.637σ and the applied shear rate was $2.346(\epsilon/m\sigma^2)^{1/2}$. The results were collected after 400 000 time steps.

A. The effect of the wall density on the wall slip

The density of the wall can be changed by adjusting the distances of the atoms from each other in X, Y and Z directions. For our simulation the size of each wall was $(9.637 \times 7.228 \times 3.253)\sigma^3$. We examined the wall slip through the velocity profile for different wall densities ranging from 1.5 to $3.0\sigma^{-3}$. For all the simulations the wall stiffness was $1000(\epsilon/\sigma^2)$. The velocity profiles in Fig. 1 show not much change in the wall slip with increasing wall density. The profiles are almost identical and there is no significant change in the wall slip for the range of wall densities examined here. This seems somehow contradictory to the results of Ref. 11; however, in that work it seems that the two densities examined for the wall are less than $1.0\sigma^{-3}$.

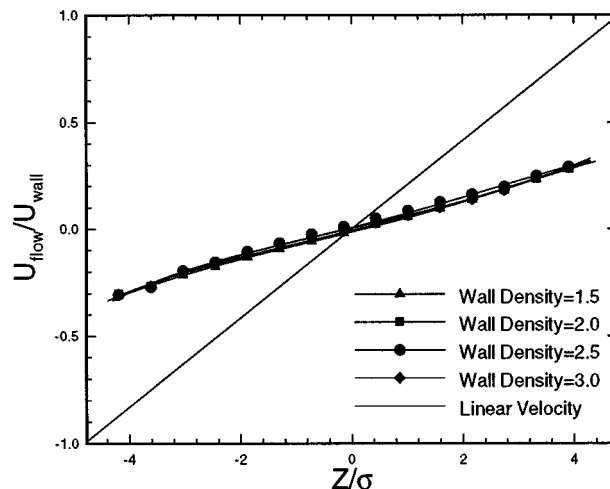


FIG. 1. Velocity profiles for different values of wall density. Shear rate is $2.346(\epsilon/m\sigma^2)^{1/2}$ and wall stiffness is $1000(\epsilon/\sigma^2)$.

Below this value a decrease in the wall density contributes to the wall roughness.¹¹ However, as we will see with a soft wall we will need to have a dense enough wall to avoid penetration of the fluid molecules at high pressures. To be on the safe side we chose to use a wall with a density of $2.5\sigma^{-3}$ for the rest of the simulations.

B. The effect of the wall stiffness on the wall slip

The springs which attach the wall atoms to their lattice sites keep the walls in the solid state. In order to examine the effect of the wall stiffness we conducted a few simulations for various values of k_w which quantify the stiffness of the walls. The wall density for all the simulations was $2.5\sigma^{-3}$. These profiles are shown in Fig. 2. As it can be seen from the profiles there is a great reduction in the wall slip as we decrease the wall stiffness. It seems that stiff walls give a great amount of wall slip. This can be explained by the fact that the wall atoms form a lattice structure. So using a very stiff spring makes them very restricted in their movement. This

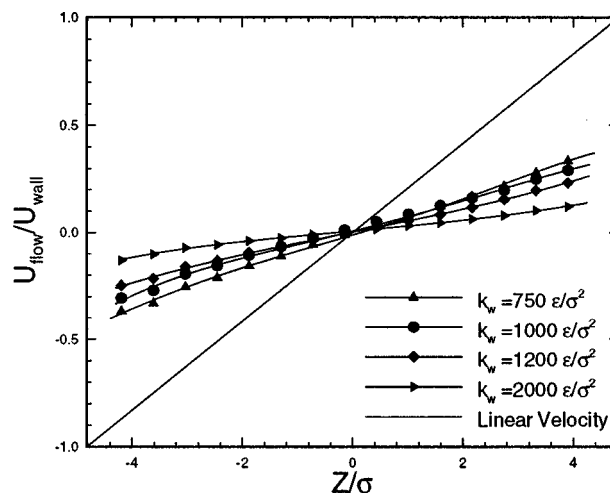


FIG. 2. Velocity profiles for various wall stiffness values. The wall density is $2.5\sigma^{-3}$ and shear rate was $2.346(\epsilon/m\sigma^2)^{1/2}$. Wall–fluid interaction strength was kept $\epsilon_w = 1.0\epsilon$ for all the simulations.

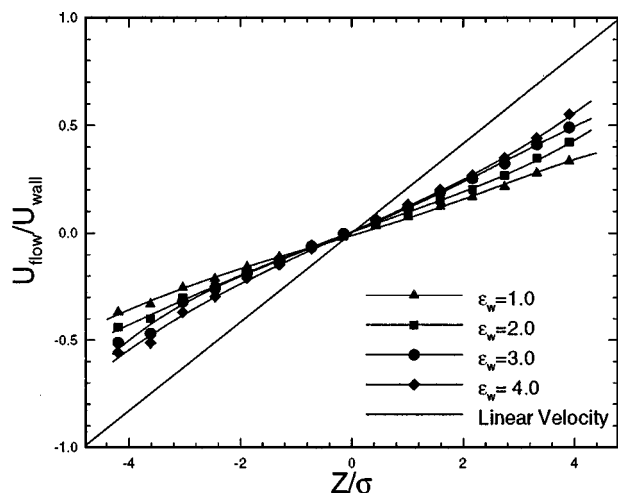


FIG. 3. Velocity profiles for different values of wall–fluid interaction strength ϵ_w . The wall density was $2.5\sigma^{-3}$ and shear rate was $2.346(\epsilon/m\sigma^2)^{1/2}$.

lack of movement makes the walls effectively smoother. In contrast, softening the springs relaxes the restriction on the movement of the wall atoms and makes them interact more efficiently with the fluid particles. This softening actually contributes to the roughness of the walls which is essential in achieving a nonslip flow. Although a slight penetration of the fluid atoms to the surface of the walls in the form of adsorption might be realistic, excessive penetration of the fluid particles causes breakdown of the simulation. The penetration of the fluid particles into the walls is strong at the high shear rates and pressures that we used in the simulation. As we decrease the stiffness of the walls the fluid particles come closer to the average position of the walls and eventually if the wall is too soft penetrate into them. For this reason it is not possible to soften the springs further than $750(\epsilon/\sigma^2)$.

C. The effect of the wall–fluid interaction strength on the wall slip

Another important wall property is wall–fluid interaction strength (ϵ_w). To study its effect on the wall slip we conducted simulations for different values of ϵ_w ranging from 1.0 to 5.0 ϵ . The stiffness of the wall was $750(\epsilon/\sigma^2)$ and the wall density was $2.5\sigma^{-3}$. The velocity profiles are shown in Fig. 3 and it can be seen that slip on the walls reduces as we increase ϵ_w . However we could not completely eliminate slip by this means.

The dependence of slip on wall–fluid interaction strength has been previously shown for LJ fluid¹⁰ and also bead-spring models of oligomers.²³ For bead-spring models it is observed that for $\epsilon_w = 1$ slip happens on the wall, however for higher values of $\epsilon_w = 2-3$, interlayer slip can be observed. From the velocity profiles with our simulation it can be seen that even at higher values of ϵ_w slip only happens on the wall. This can be attributed to the different model of molecules used in our simulations. As with similar alkane simulations¹² with similar wall–fluid interaction strength it is seen that the slip mostly happens on the wall. Another important difference in our simulations and that

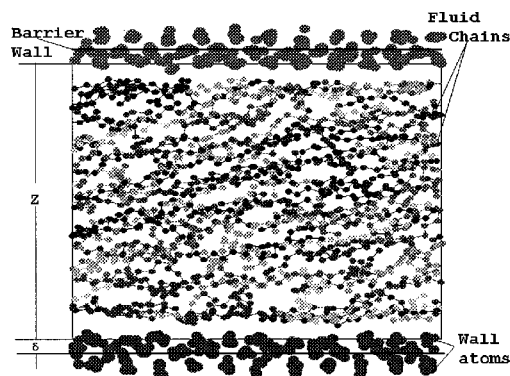


FIG. 4. Simulation box in XZ plane. Two walls are separated by z . The position of the barrier wall is indicated by a thick line. The atoms with the same shade belong to the same molecule.

used with bead-spring models is the temperature. The temperature used with a bead-spring model in Ref 23 is $T = 1 \epsilon/k_B$. If we use the value of ϵ corresponding to hexadecane it will be $T = 50.5$ K, which is very low temperature compared to what we have used here. We will also see that the adsorption of the molecules onto the surface becomes easier with a rougher surface. In that case with an energetic enough surface slip can happen between the fluid layers.

IV. DEVISING A NEW MODEL FOR THE WALL

From the results obtained in Sec. III it can be concluded that the wall density in the range examined here has little effect on the slip. Both wall stiffness k_w and wall–fluid interaction strength ϵ_w significantly affect wall slip. But with the current model there is a limit to the softness of the walls. At the same time increasing ϵ_w to much higher values changes the configuration of the fluid and might result in solidification of fluid particles near the walls,¹⁰ although we are often more interested in simulating the film in its liquid state. So we decided to modify our model for the wall in a way that makes it possible for us to soften the wall further. This softer wall would not represent a stiff wall like mica where the mean displacement of the wall atoms must be within the Lindeman criterion. Rather, it will provide the possibility of economically simulating shear flow with less slip when this is desired. The results can then be qualitatively compared with experiments with mica. It is in some ways similar to using a hydrocarbon¹² wall which is not actually a solid physical wall, but occurs in practice due to adsorption of short chain molecules onto a solid surface.

A. Barrier wall

In Sec. IIIB we saw that the penetration of the fluid particles into the wall was the reason that we could not soften the wall further. In order to solve this problem we introduce a new wall which we call a barrier wall. Figure 4 shows a snapshot from the simulation box and proposed position of the barrier wall, the chains of hexadecane as fluid particles and also the wall particles. The snapshot is taken for a wall stiffness value $k_w = 750(\epsilon/\sigma^2)$. As it can be seen from the snapshot there is a depletion zone which is a familiar phenomenon with frozen atomic walls. We believe this

depletion zone contributes to the slip by decreasing the apparent wall roughness and the cohesion between the wall and the fluid. We implemented the barrier wall into the model in the following way. Two structured walls of the type previously described are separated by a distance of z and the origin is in the center of the simulation box. One barrier wall is located at each side in the Z direction in locations $\pm(z/2 + \delta)$. δ is the offset of the barrier wall. This offset makes it possible for the fluid particles to engage with the wall particles and penetrate just slightly in the wall. Barrier walls have a potential of the form

$$\phi = 0.0002\pi e \left[\frac{2}{5} \left(\frac{\sigma}{z} \right)^{10} - \left(\frac{\sigma}{z} \right)^4 \right]. \quad (6)$$

This potential originally is the integration result of a 6–12 Lennard-Jones potential on a XZ plane of a fcc lattice,²⁴ and is additional to the potential of the atoms of the structured wall. We have modified the original potential by removing the long range attractive part of the potential and making the potential much weaker. The potential and the force exerted on the fluid particles depend only on the normal distance of the fluid particles from the barrier wall (z). The barrier wall's potential is cut off at a distance of 0.2σ so that it exerts a normal force only on the particles which are about to penetrate into the structured walls. This strategy makes it possible to solve the penetration problem. The barrier wall actually acts as a layer of atoms arranged in a fcc lattice and frozen in their lattice sites.

B. The velocity profiles with the new wall model

To test the effectiveness of the newly devised wall we repeated the simulation for a system with walls separated by 9.637σ . The same high shear rate as in Sec. III of $2.346(\epsilon/m\sigma^2)^{1/2}$ was also applied. The wall stiffness used this time was $k_w = 75(\epsilon/\sigma^2)$. This is ten times softer than the softest walls we were able to use without the barrier wall in Sec. III B. The wall–fluid interaction strength was $\epsilon_w = 1.0\epsilon$. To demonstrate the effect of softening the walls with the implementation of the barrier wall we took another snapshot with the same shear rate and wall fluid interaction strength as in Fig. 4. This is shown in Fig. 5. It can be seen that letting

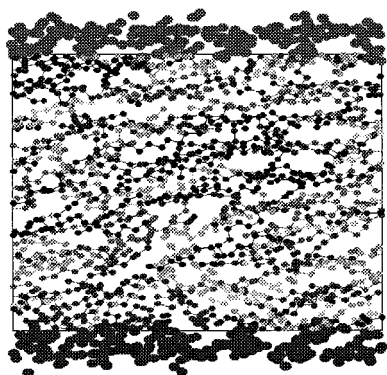


FIG. 5. A snapshot from the simulation box in the XZ plane with barrier walls implemented into the model. The wall stiffness is reduced to $75(\epsilon/\sigma^2)$.

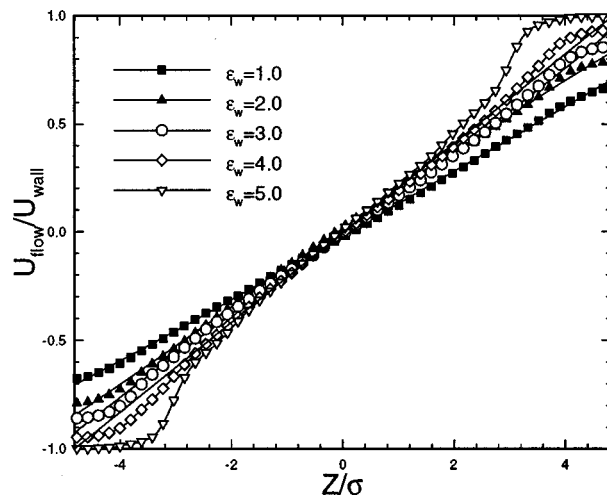


FIG. 6. Velocity profiles for a system of walls separated by 9.637σ after implementing the barrier wall and softening the wall stiffness to $75(\epsilon/\sigma^2)$. The solid line is the ideal linear velocity profile.

the wall stiffness relax makes the fluid particles come closer to the average position of the walls. In a physical sense this increases the roughness of the wall and contributes to engagement between the fluid and wall particles. We observed no difficulty in the simulation and the results proved that the method used resulted in a decrease in the wall slip. Although the reduction in the wall slip was significant it did not cause the wall slip to disappear completely. In simulations with tetracosane and squalane¹² it is also observed that letting the fluid particles penetrate into the tethered chains on the wall by reducing surface coverage of tethered chains is effective in reducing the slip. To see if we could reduce the slip further, we decided to increase the value of ϵ_w . We did several simulations with various values for ϵ_w ranging from 1.0 to 5.0 ϵ . The velocity profiles are presented in Fig. 6. For this particular shear rate it seems that with $\epsilon_w = 4\epsilon$ we obtain a velocity profile very close to linear and with only a very small amount of slip (of about 5%) of the wall velocity. The density profiles for this simulation are shown in Fig. 7 where it can be seen that up to $\epsilon_w = 4\epsilon$ the density profiles remain

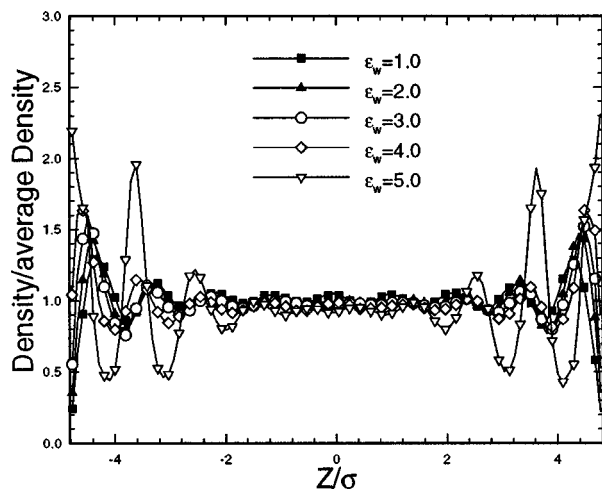


FIG. 7. Density profiles for the simulated system described in Fig. 6.

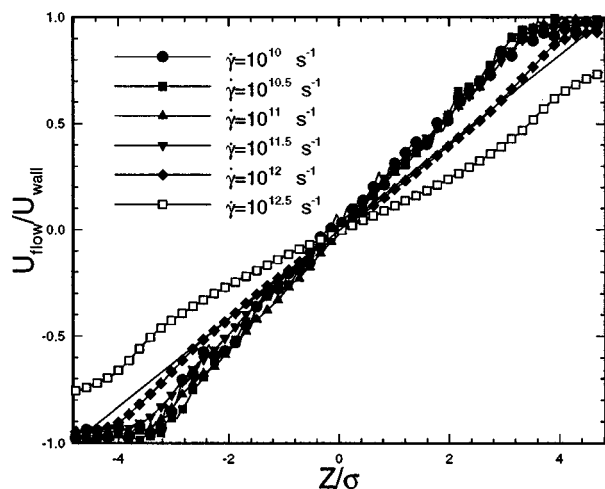


FIG. 8. Velocity profiles for a strong adsorbing surface where $\epsilon_w = 4\epsilon$. Various shear rates ranging from 10^{10} to $10^{12.5} \text{ s}^{-1}$ are covered in these simulations. The film thickness is 9.637σ .

almost the same. The density profile changes drastically at $\epsilon_w = 5\epsilon$ and it shows an enhanced layering effect in the fluid structure. This layering effect is the characteristic of confined films. At this point we can see that the first layer is stuck to the wall and the slip plane is moved inside the film.

V. THE EFFECT OF SHEAR RATE ON THE SLIP

A. The effect of the shear rate with a strongly adsorbing wall

In experiments with mica and other surfaces which are considered as strong adsorbing surfaces, many layers of the confined fluid can be immobilized by adsorption onto the solid surfaces. ϵ_w/k_B for mica is approximately 360–600 K which is 7–10 times larger than ϵ/k_B .²⁵ Another approximation in the literature for the ϵ_w of mica is 3–5 ϵ , which is considered to be conservative.²⁶ The surface energy of gold is approximately 3 ϵ .²⁷ Other metal surfaces are also less attractive than mica.²⁸ The exact definition of a strongly adsorbing surface in terms of ϵ_w is rather arbitrary. However some researchers²³ consider $\epsilon_w \leq 1.0\epsilon$ as weakly adsorbing and $\epsilon_w = 2-3\epsilon$ as a strongly adsorbing surface; the simulations in Ref. 23, as mentioned above, are conducted at very low temperatures not applicable to real lubrication problems. Considering the values of ϵ_w for mica, gold and other metals we chose $\epsilon_w = 4\epsilon$ to simulate a strongly adsorbing surface close to typical surfaces used in real applications. The response of such systems to wall slip in shear flow is important in determining the effective shear rate and the position of the shear plane.

We have carried out the simulations at different shear rates of $0.0234-7.418 (\epsilon/m\sigma^2)^{1/2} (10^{10}-10^{12.5} \text{ s}^{-1})$. From the results shown in Fig. 8 it can be seen that at lower shear rates up to $10^{11.5} \text{ s}^{-1}$ many layers of the hexadecane molecules are stuck to the solid surface. Increasing shear rate however causes slip between the solid and fluid layers. This slip increases with the shear rate. This may be better explained by looking to the density profiles in Fig. 9 for these shear rates. The large peaks in the density profiles close to

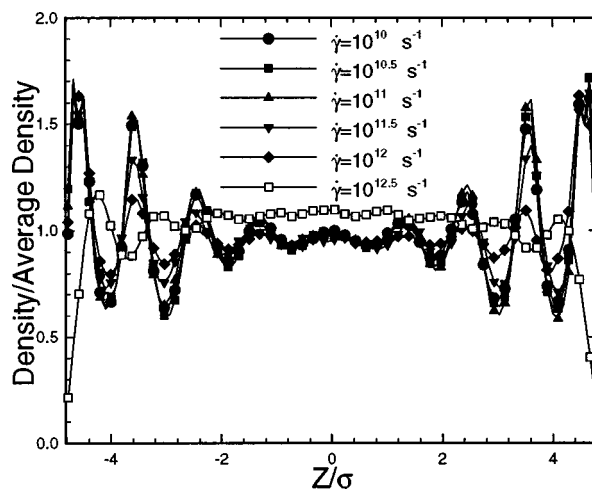


FIG. 9. Density profiles for various shear rates ranging from 10^{10} to $10^{12.5} \text{ s}^{-1}$ for a strong adsorbing surface where $\epsilon_w = 4\epsilon$.

the walls indicate strong adsorption on the walls. Density profiles remain almost unchanged up to a shear rate of $10^{11.5} \text{ s}^{-1}$. However increasing the shear rate further lowers the peak density in the adsorbed layers. This change is much more dramatic for the highest shear rate where most of the adsorbed layers are washed away to the center. This results in a sudden increase in the slip which is observed in the velocity profiles.

B. The effect of the shear rate with a weak adsorbing wall

In the experiments conducted with surface force apparatus (SFA) a thin film of liquid lubricant or polymeric solution or melt is usually confined between two crossed cylinders of muscovite mica. Mica itself is a strongly adhesive material.²⁶ However, in experiments conducted for low adsorbing surfaces the mica surface is coated with a layer of octadecyltriethoxysilane (OTE).²⁶ The result was a surface many times less adsorbing than the mica itself. Although the model wall here does not represent the mica atom by atom, the surface energy of the model wall can be adjusted to a level similar to that of a coated surface in the experiments. In order to have slip results for this weakly adsorbing surface we conducted simulations for different shear rates ranging from $10^{9.75}$ to $10^{12.5} \text{ s}^{-1}$.

The effective shear rate ($\dot{\gamma}_{\text{eff}}$) can be calculated inside the film from the velocity profiles. The ratio of $\dot{\gamma}_{\text{eff}}/\dot{\gamma}$ is an indicator of degree of slip. We define the degree of slip (S) as the ratio of the slip velocity to apparent velocity and this is

$$S = \frac{V_s}{V_{\text{app}}} = \frac{V_{\text{app}} - V_{\text{eff}}}{V_{\text{app}}} = 1 - \frac{\dot{\gamma}_{\text{eff}}}{\dot{\gamma}}. \quad (7)$$

A value of $S > 0$ indicates slip boundary condition holds and for $S = 0$ a nonslip condition prevails. Table II shows $S = 1 - (\dot{\gamma}_{\text{eff}}/\dot{\gamma})$ for various shear rates for this film thickness. It can be seen that increasing the shear rate leads to an interesting phenomenon different from that with strongly adsorbing surfaces. In this case the largest degree of slip was seen

TABLE II. Degree of slip (S) for various applied shear rates. The film thickness for all the simulations is 3.898 nm and wall–fluid interaction strength is $\epsilon_w = \epsilon$.

$\log(\dot{\gamma})$	9.75	10	10.5	11	11.5	12	12.25	12.5
S	0.674	0.654	0.647	0.610	0.443	0.322	0.336	0.565

at the lowest shear rate of $10^{9.75} \text{ s}^{-1}$. It can be seen that the slip is large at low shear rates with values closer to 1 for S . As the shear rate is increased S is decreased as an indication of decrease in the slip. However S never reaches zero (non-slip condition) and there is a turning point at shear rates of around 10^{12} s^{-1} . At this point the slip intensifies again and S increases as we increase the shear rate further.

Again, to demonstrate the effect of the adsorption in the observed phenomenon let us look at the density profiles in Fig. 10 for the simulated shear rates at this weakly adsorbing surface. From Fig. 10 it can be clearly seen that increasing the shear rate up to 10^{12} s^{-1} pushes the adsorbed layers toward the walls. This can be better observed in the center where the average density of the fluid is decreased as we increase the shear rate, which is the main reason why slip is decreased in this range of shear rate. After this point as we increase the shear rate further the high velocity of the walls washes the adsorbed layers away from the walls toward the center. This results in an increase in the density profiles in the central region and reduces the adsorption level on the surfaces which is the main cause of enhanced slip.

Theoretical works by Subbotin *et al.*²⁹ on the shear response of polymer melts confined between weakly adsorbing surfaces support our findings. We must emphasize the fact that although the length of polymer melt molecules can be much longer than the shorter chains of alkanes and the shear rates used in the theory seem to be lower, existing similarities and the lack of any other theoretical analysis for shorter chains make the mentioned theoretical work currently the best possible explanation for the observed phenomenon.

In this theoretical work²⁹ two characteristic shear rate are defined, namely $\dot{\gamma}_1$ and $\dot{\gamma}_2$. The amount of slip is large

when $\dot{\gamma} < \dot{\gamma}_1$ and when $\dot{\gamma}_1 < \dot{\gamma} < \dot{\gamma}_2$ slip decreases and for shear rates $\dot{\gamma} > \dot{\gamma}_2$ the slip becomes negligible. Our findings fit in well with this theoretical prediction except at high shear rates. Considering our results and their analogy it seems that the first characteristic shear rate is at $\dot{\gamma}_1 \approx 10^{9.75} \text{ s}^{-1}$ or somewhat lower. However, we do not reach the second characteristic shear rate $\dot{\gamma}_2$ and increasing the shear rate beyond 10^{12} s^{-1} results in further increase in the slip. The reason for this difference is not clear. However it might be due to the specific model we have used here with relatively short chains (in comparison to long polymer melt chains) combined with high shear rates used in the simulation. Or there might be some fault in the theoretical prediction. It seems more investigations at high shear rates, maybe through experiments or more simulations with longer chains, should be done to clarify this matter. We think however that at shear rates lower than 10^{12} s^{-1} the simulation and theoretical results agree well. For polymer melts in Ref. 29 the slip is larger for small shear rates where the chains are still close to Gaussian. The elongation of the chains at higher shear rates leads to compression of the polymer melt and a decrease in the slip.²⁹ In our case the chains are shorter but we observe the same phenomenon. At much higher shear rates since the chains are already fully stretched the chain elongation factor will not be as strong as before and hence the slip will be intensified. This could be considered as a possible explanation for different behavior from the theory at higher shear rates.

Our results are somewhat in contradiction with the results obtained for bead-spring models with 6–10 segments per chain²³ confined between two rigid atomic walls. In this work²³ with a similar value for ϵ_w an increase in the shear rate leads to a further increase in the slip on the wall while inside the film the induced shear rate remains the same. This discrepancy can only be explained by very low temperatures used in bead-spring simulations. Also the chains in our simulations are longer and are modeled more realistically. Another explanation for this difference lies in the fact that the walls in our simulations are effectively rougher and an increase in the shear rate leads to larger normal stress differences¹³ that compress the fluid against the walls. With effectively a rough wall this leads to a better engagement between the wall and the fluid and results in a decrease in the slip.

There have been experimental slip measurements for polymers by Migler and his co-workers.² However their measurements are done at considerably smaller shear rates ($2 \times 10^{-2} - 40 \text{ s}^{-1}$) and with much thicker films. They measured the slip velocity within the first 100 nm from the solid–liquid interface and found that the slip will increase with increasing shear rate. This however can be explained by the fact that their system can be considered as one of the

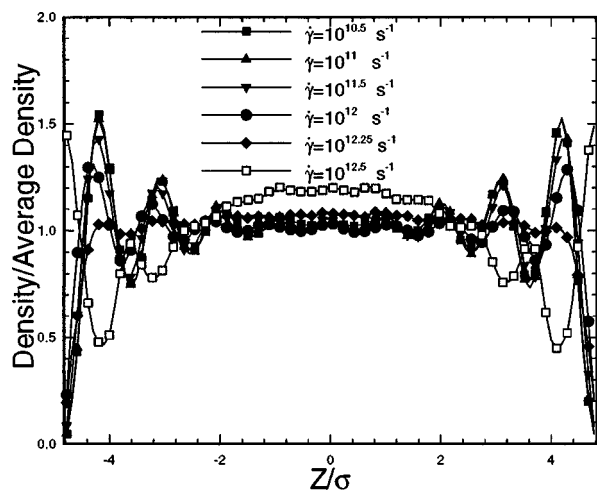


FIG. 10. Density profiles for various shear rates ranging from $10^{10.5}$ to $10^{12.5} \text{ s}^{-1}$ for a weak adsorbing surface where $\epsilon_w = \epsilon$.

TABLE III. Degree of slip (S) for various film thicknesses. The shear rate ($\dot{\gamma}$) for all the data here is $10^{11.5} \text{ s}^{-1}$ and wall–fluid interaction strength is $\epsilon_w = \epsilon$.

Z (nm)	0.975	1.949	2.924	3.898	4.873	5.848	6.822	19.490
S	0.844	0.718	0.553	0.443	0.385	0.325	0.287	0.136

thick films close to the bulk state of the fluid. To demonstrate the effect of the thickness of the film on the slip we conducted a few simulations which are explained in Sec. V B 1.

1. The effect of the film thickness on the slip

Several simulations were performed with various film thicknesses ranging from 2.409σ to 48.186σ (0.9745–19.4915 nm). The shear rate was kept constant at $0.7418 (\epsilon/m\sigma^2)^{1/2}$ for all the simulations. We calculated the degree of slip given by Eq. (7) for those thicknesses. The results are shown in Table III.

At the thickest film of 19.490 nm (48.187σ) the slip velocity is only 14% of the wall velocity. For thinner films the slip is larger and for a film with a thickness of 3.898 nm (9.637σ) the slip velocity amounts to about 44% of the wall velocity. This is a significant increase in the slip. From the results it can be inferred that S approaches zero at thick enough films. This suggests that with a very thick film a nonslip boundary condition holds. The point that the slip is thickness dependant is very significant and should be considered in experiments. These results are similar to the results for longer molecules of squalane and tetracosane¹² and we speculate that this phenomenon is independent of the molecular architecture, since that squalane is a branched molecule. It seems it is also independent of the type of the model wall as in a constant load simulation of hexadecane¹¹ with rigid walls it was inferred that the slip is decreased at thicker films.

In our discussion on the experimental findings of Migler and his co-workers,² it was demonstrated that the slip decreases at thicker films for the same shear rate. Their measurement cannot be directly compared with a thin film which is only about 10 segment diameters thick. However future research agenda can accommodate the examination of the shear dependence of slip in the weak adsorption limit for much thicker films through molecular simulation. But since such a simulation requires much longer times to yield the results it was not conducted in this work. The physical explanation for observing this phenomenon is still open for discussion.

VI. CONCLUSIONS

Here we examined the shear flow of hexadecane between two solid walls. We demonstrated the effect of the detailed properties of a model wall on the slip between hexadecane and a solid surface. It was found that the slip between fluid and the wall depends on both the wall–fluid interaction strength and surface roughness which in our model was controlled by the wall stiffness. A model was devised based on our findings. The slip was examined at various shear rates and for films of different thicknesses. The results are ana-

lyzed at different values for the wall–fluid interaction strength ϵ_w which determines the level of adsorption of the fluid molecules onto the solid surface. It was demonstrated that the slip depended on shear rate and film thickness. However different behavior was observed depending on the level of adsorption which was dictated by the wall–fluid interaction strength. The degree of slip is found to be smaller for thicker films. The choice of ϵ_w has a great effect on both the wall slip velocity and fluid density distribution in the direction normal to the wall. Using $\epsilon_w = 4\epsilon$ can be considered a reasonable value for ϵ_w if a comparison with strongly adsorbing surfaces is to be made. The simulation was also used to yield some results for comparison with what has been obtained by experiments for low adsorbing surfaces, similar to those used with OTE coated mica surfaces. In this case a lower value for ϵ_w would be more appropriate and should be chosen depending on the surface energy of the material. It was demonstrated that the level of adsorption of the molecules onto the surface is a determining factor for slip. This was true for both strong and weak adsorbing surfaces and was discussed in detail from the density profiles. Although the simulated hexadecane molecules are much shorter than typical polymer melt molecules close similarities in behavior can be seen. The effect of the surface interaction energy ϵ_w on the rheological properties of the confined films of n -hexadecane has also been investigated for a better understanding of the problem.¹³

ACKNOWLEDGMENTS

The authors gratefully acknowledge the support of an Australian Research Scheme grant for this work. They also wish to thank Professor N. Phan-Thien for providing them with generous time on the computing facility of the Sydney Distributed Computing Laboratory (SyDCom).

¹M. Sun and C. Ebner, Phys. Rev. Lett. **69**, 3491 (1992a).

²K. B. Migler, H. Hervet, and L. Leger, Phys. Rev. Lett. **70**, 287 (1993).

³P. G. de Gennes, C. R. Seances Acad. Sci. Ser. B **288**, 219 (1979).

⁴J. R. A. Pearson and C. J. S. Petrie, *Polymer Systems: Deformation and Flow, Proceedings of the Annual Conference of the British Society of Rheology*, edited by R. E. Wetton and R. W. Whorlow (Macmillan, New York, 1968), p. 163.

⁵D. Dowson, *Thin Films in Tribology*, Proceedings of the 19th Leeds-Lyon Symposium on Tribology (Elsevier, New York/Amsterdam, 1993), pp. 3–12.

⁶D. K. Bhattacharya, Phys. Rev. A **43**, 761 (1991).

⁷M. Sun and C. Ebner, Phys. Rev. Lett. **46**, 4813 (1992b).

⁸P. A. Thompson and G. S. Grest, Phys. Rev. Lett. **68**, 3448 (1992).

⁹P. A. Thompson and M. O. Robbins, Phys. Rev. A **41**, 6830 (1990).

¹⁰A. Jabbarzadeh, J. D. Atkinson, and R. I. Tanner, J. Non-Newtonian Fluid Mech. **69**, 169 (1997).

¹¹M. J. Stevens, M. Mondello, G. Grest, S. T. Cui, H. D. Cochran, and P. T. Cummings, J. Chem. Phys. **106**, 7303 (1997).

¹²S. D. Gupta, H. D. Cochran, and P. T. Cummings, J. Chem. Phys. **107**, 10316 (1997).

- ¹³A. Jabbarzadeh, J. D. Atkinson, and R. I. Tanner, *J. Non-Newtonian Fluid Mech.* **77**, 53 (1998).
- ¹⁴P. J. Daivis, D. J. Evans, and G. P. Morriss, *J. Chem. Phys.* **97**, 616 (1992).
- ¹⁵S. Chynoweth and Y. Michopoulos, *Mol. Phys.* **81**, 133 (1994).
- ¹⁶S. Chynoweth, U. C. Klomp, and L. E. Scales, *Comput. Phys. Commun.* **62**, 297 (1991).
- ¹⁷R. K. Ballamudi and I.A. Bitsanis, *J. Chem. Phys.* **105**, 7774 (1996).
- ¹⁸S. Gupta, D. C. Koopman, G. B. Westermann-Clark, and I. A. Bitsanis, *J. Chem. Phys.* **100**, 8444 (1994).
- ¹⁹J. H. R. Clarke and D. Brown, *Computer Simulation of Polymers*, edited by E. A. Colbourn (Longman Scientific & Technical, Essex, England, 1994), pp. 47–90.
- ²⁰J. P. Ryckaert and A. Bellemans, *Chem. Phys. Lett.* **30**, 123 (1975).
- ²¹P. van der Ploeg and J. C. Berendsen, *J. Chem. Phys.* **76**, 3271 (1982).
- ²²A. Jabbarzadeh, J. D. Atkinson, and R. I. Tanner, *Comput. Phys. Commun.* **107**, 123 (1997).
- ²³E. Manias, G. Hadziioannou, and G. ten Brinke, *Langmuir* **12**, 4587 (1996).
- ²⁴S. A. Somers and H. T. Davis, *J. Chem. Phys.* **96**, 5389 (1992).
- ²⁵R. Ballamudi and I. A. Bitsanis, *Mater. Res. Soc. Symp. Proc.* **336**, 123 (1995).
- ²⁶J. Peanasky, L. L. Cai, and S. Granick, *Langmuir* **10**, 3874 (1994).
- ²⁷T. K. Xia, J. Ouyang, M. W. Ribarsky, and U. Landman, *Phys. Rev. Lett.* **69**, 1967 (1992).
- ²⁸E. Pelletier, J. Montfort, J. Loubet, A. Tonck, and J. Georges, *Macromolecules* **28**, 1990 (1995).
- ²⁹A. Subbotin, A. Semenov, G. Hadziioannou, and G. ten Brinke, *Macromolecules* **28**, 3901 (1995).